Journal of Molecular Liquids 340 (2021) 116841

Contents lists available at ScienceDirect

Journal of Molecular Liquids

journal homepage: www.elsevier.com/locate/molliq

# Unusual ion transport behaviour of ethylammonium nitrate mixed with lithium nitrate

Andrei Filippov [a,b,*], Artem S. Alexandrov [c], Rustam Gimatdinov [b], Faiz Ullah Shah [a,*]

[a] Chemistry of Interfaces, Luleå University of Technology, SE-97187 Luleå, Sweden
[b] Kazan State Medical University, 420012 Kazan, Russia
[c] Kazan Federal University, 420008 Kazan, Russia

ARTICLE INFO

*Article history:*
Received 23 March 2021
Revised 25 May 2021
Accepted 25 June 2021
Available online 1 July 2021

*Keywords:*
Protic ionic liquids
Diffusion
Ion dynamics
Phase transformations
Effect of magnetic field

ABSTRACT

The diffusivity of ions and ionic conductivity of ethylammonium nitrate (EAN) mixed with lithium nitrate ($LiNO_3$) has been carried out as a function of Li-salt concentration and temperature. An unusual behavior of ion diffusivities and ionic conductivities of the mixtures are observed over a range of Li-salt concentration and temperature. The diffusivities of $EA^+$ and $Li^+$, as measured by pulsed-field gradient (PFG) nuclear magnetic resonance (NMR) diffusometry, are found to be comparable in the lower temperature range. An overall decrease in the ion diffusivity is observed with an increase in the concentration of $LiNO_3$. A lower degree of dissociation of ionic complexes in the presence lower concentration of the Li-salt (less than 6 mol. %) resulted in lower ionic conductivity. In the higher concentration range of Li-salt the $Li^+$ diffusivity is monotonously decreased with an increase in the concentration. In the lower concentration range, the $Li^+$ diffusivity exceeded the diffusivity of $EA^+$ cation demonstrating the release of $Li^+$ from the associates. Being enclosed between glass plates, the diffusivities of $EA^+$ and $Li^+$ showed peculiarities similar to the earlier observed results for neat nitrate ILs: accelerated diffusivity of cations and reversible alteration of diffusivities under the influence of strong static magnetic field.



## 1. Introduction

Ionic liquids (ILs) have been widely used in a range of applications due to their unique physicochemical and electrochemical properties including high thermal and electrochemical stability, non-flammability, negligible vapor pressure, high ionic conductivity and electrochemical stability window [1–5]. There is an excellent opportunity to design and synthesize new ILs for any specific application because of their structural designability [3]. Synthesis is just one of the approaches to produce new systems with desirable properties, while another simpler and promising way is to use ILs in a composite system. ILs can be used with the addition of organic and inorganic chemical compounds or other types ILs, allowing to change the interactions of anions and cations, and ultimately obtaining the required set properties appropriate for the task at hand [4]. In electrochemistry, the use of additives in ILs have come to the forefront. In the case of pure ILs, there is a significant ionic association or aggregation leading to high viscosity and low ionic conductivity. The introduction of new substances into an IL might decrease the Coulomb interactions by releasing the ions from associates and aggregates, which will lead to a decrease in viscosity, an increase in ion diffusivity and ionic conductivity [6].

Ethylammonium nitrate (EAN) is the first room-temperature IL, which was identified and characterized by Walden in 1914 [7]. EAN has several useful properties making it a promising candidate for various applications. It is an excellent solvent and has proven itself well with proteins. The proteins treated with EAN were more stable than the proteins treated with traditional organic solvents [8]. In addition, it was shown that EAN can prevent aggregation of denatured protein [9]. EAN is a transparent, colorless, odorless liquid and can form micelles when surfactants are added to it [10] and, like water, forms three-dimensional networks of hydrogen bonds [11,12]. Like other protic ILs, EAN has an electrochemical stability window of 3.45 V and can be used in a range of electrochemical devices [13,14].

The structure of EAN was determined by its amphiphilic nature and the hydrogen bonding capability that leads to an extended network across the polar region [12,15]. Using density functional method, it was possible to obtain a three-dimensional model of the structure of hydrogen bonds in an

* Corresponding authors at: Chemistry of Interfaces, Luleå University of Technology, SE-97187 Luleå, Sweden (A. Filippov).
*E-mail addresses:* andrei.filippov@ltu.se (A. Filippov), faiz.ullah@ltu.se (F. Ullah Shah).

https://doi.org/10.1016/j.molliq.2021.116841
0167-7322/

EAN [16]. Unlike water, the EAN bond system does not have a tetrahedral character due to the presence of donor–acceptor mechanisms of bond between the ions. The nitrate anion in EAN has a planar configuration; it consists of three oxygen atoms symmetrically located around the central nitrogen atom. Through oxygen atoms, the $NO_3^-$ ion binds to the protons of amino group $NH_3$ due to the formation of hydrogen bonds and electrostatic interaction, while adjacent cationic alkyl chains join through hydrophobic interactions, resulting in a continuous (bicontinuos) "spongy" structure [17]. Thus, the formation of hydrogen bonds occurs in the structure of the EAN, the order of which is preserved up to distances exceeding 10 Å [18]. While studying of the structure of the EAN by computer simulation methods, it was found that in most cases the amino group, having three donor protons, forms bonds simultaneously with three anions [19]. In addition, not all acceptor oxygens of the anion take part in hydrogen bonds. In 30% of cases, one oxygen binds to two cations at once, the other two oxygen of the anion may remain unpaired. It was also shown that sometimes the formation of "ring" structures occurs. Atkin and Warr have investigated nano-scale segregation of short chain ILs, PAN nitrate and EAN, by SANS [20] and have found the evidence of structural heterogeneity in these ILs, where "solvophobic interaction" is the most important factor. This result provides an experimental evidence of nano-scale heterogeneity in the ILs with alkyl chains shorter than $C_4$. The calculated Bragg spacings are approximately twice the ion pair dimensions of the ILs, which suggests that the ILs are structured on the length scale of the ions, with the alkyl groups associated together and segregated from the H-bonded ionic moieties - $ND_3^+$ and $NO_3^-$.

It was demonstrated that dissolution of EAN in water at different concentrations changes the transport and thermodynamic characteristics of the solution [6]. The highest conductivity was observed at the molar concentration of EAN less than 20%. Solvation of EAN ions by water molecules weakens the Coulomb interactions and hydrogen bonding interactions between the oppositely charged ions, and as a result leading to a decrease in viscosity and an increase in the ionic conductivity due to the increase in charge carriers. Such aqueous solutions can be used as electrolytes in supercapacitors and fuel cells. A similar effect was observed in another study, where the addition of EAN to organic solvents such as formamide and dimethyl carbonate showed a significant effect on the characteristics of the solution [21]: at specific concentrations of the constituent components, a decrease in viscosity and an increase in ionic conductivity were observed. Several studies were devoted to the dynamic properties of ILs with dissolved inorganic salts. It was shown that the ionic conductivity of such solutions changes with the salt contents and reaches a maximum at a certain concentration [22–24]. This is due to the complexity of interactions between the IL ions and the salt ions: the ordered structure of the IL is destroyed, and the ions become more mobile upon the addition of solvents.

The addition of $LiNO_3$ salt to EAN has been of special interest to various researchers [13,15,25,26]. The understanding of lithium ion solvation and transport in ILs is important due to their promising applications in electrochemical devices. It was assumed that the presence of salt should change the microstructure and various characteristics including translational mobility and electrical conductivity of the IL. At ambient conditions, $LiNO_3$ is miscible in EAN up to ~ 0.2 M fraction [15]. A study on $Li^+$ solvation and diffusion in EAN has been performed by ab initio molecular dynamics calculations based on density functional theory [13]. The local structure of EAN around the lithium cation has been analyzed that showed that the lowest two free energy minima correspond to conformations with the $Li^+$ being solvated either by three or four nitrate ions with a transition barrier of 0.2 eV between them [13]. It was proposed that in such a system an associate of IL and a lithium ion is formed [5,27]. The viscosity of such a system increases and the electrical conductivity decreases in the presence of a salt [27].

The effect of a $LiNO_3$ salt on the morphology of EAN was studied by X-ray diffraction and molecular dynamic simulations [15,28]. The results showed that the IL retains its structure upon addition of salt, and the violation of the interactions between the ammonium group of the cation and the nitrate anion turned out to be insignificant [15]. The $Li^+$ are distributed in the charged domains where they undergo a further level of self-segregation. Small amount of $Li^+$ ion tends to segregate into EAN's polar domains with a tendency to create solid-like $LiNO_3$ clusters with $LiNO_3$ separation at higher salt content. The effect of the added $LiNO_3$ to EAN has been investigated by rheology and colloidal probe AFM [25]. The rheology has shown a complex viscosity dependence on $Li^+$ concentration, while AFM force curve revealed a step that broadened in the presence of $Li^+$. Both these effects have been ascribed to bulk nanostructures.

Recently, the so-called nanostructured solvation paradigm has been formulated, according to which selective solvation takes place in ILs with polar (apolar) solutes going to the polar (apolar) nanoregions of the liquid [26]. Particularly, metal salts dissociate in ILs and their polar constituents go to the polar regions of the mixture forming ligand–metal complexes. NMR studies demonstrated that the influence of the addition of salt on the chemical shifts of the signals associated to hydrogen atoms in the apolar regions of the protic IL is negligible [26]. Diffusion coefficients of lithium cation support the conclusion that $Li^+$ diffusion takes place inside the anhydrous complexes [26]. In the wet IL, the signal of the water protons (4.66 ppm) is slightly shifted upfield ($-\delta$) relative to that of protons in pure water that is present at 4.807 ppm [26] in $H_2O/D_2O$ mixtures, while in the dried sample the opposite is found. This reveals that the shielding of the water protons in the IL environment is stronger than that in pure water, which is associated to weaker hydrogen bonding in the significantly micro-heterogeneous mixtures. However, as the number of water molecules decreases, the protons are more strongly deshielded by the ionic species in the bulk. It was shown experimentally [29] and by simulations [30] that strong cation − anion interactions in a wide range of lithium-salt/IL mixtures may result in a negative lithium transference number. Despite the enormous efforts, the complexity of $Li^+$ solvation and its mobility in the viscous EAN structure has not been yet fully unraveled.

The ILs inside different type of confinements, particularly micrometer-scaled [31–37], have attracted the attentions of researchers. The neat EAN and EAN-water mixtures were thoroughly investigated [32,35,38–40]. Magnetic field is an important external factor, which is present in personal electronics and industrial devices, influences the physical phase state and dynamic properties of the confined EAN [38,40–42]. An enhanced diffusivity of cations as well as an accelerated NMR relaxation of —$NH_3$ protons have been observed for EAN confined in the layers with a thickness of about 4 μm between glass plates [35,41]. One of the main factors responsible for this effect is the hydrogen-bond network [35,38,40]. An exposure to the strong static magnetic field of an NMR spectrometer leads to a gradual decrease in diffusivity of ions until it reaches an equilibrium value near that of the bulk EAN [38].

The understanding the ion transport mechanisms and molecular associates is of great importance not only in Li-ion batteries and fuel cells but also in many other systems. In this work, we study the ion diffusivity as well as ionic conductivity $LiNO_3$ dissolved in EAN. We further investigate the effects of a magnetic field on the diffusivity of EAN as well $Li^+$ ions in EAN/$LiNO_3$ mixtures enclosed between glass plates.

## 2. Materials and methods

### 2.1. Sample preparation

Ethylammonium nitrate (EAN) was synthesized and characterized as reported previously [35]. The water content in the synthesized EAN was less than 0.05 wt% as determined by Karl-Fisher titration (Metrohm 917 Karl Fisher Coloumeter with HYDRANAL reagent). $LiNO_3$ (>99%) was purchased from Sigma-Aldrich and used as received. The mixtures were prepared by weighting the two compounds in an Eppendorf tube inside a glove box at dry atmosphere followed by thorough mechanical mixing and sonication in the water bath. All the samples were additionally vacuummated during 24 h.

Samples with enclosed EAN were prepared with thin borosilicate glass plates (0.1 × 2.5 × 14 mm), Thermo Scientific Menzel-Gläser, Menzel GmbH, Germany. The glass plates were carefully cleaned before use. A stack of glass plates containing EAN or mixture EAN with $LiNO_3$ was prepared in a glove box in a dry nitrogen atmosphere. Samples were prepared by adding 1 μL of the liquid to the first glass plate, placing a second glass plate on top, adding 1 μL to this glass plate, etc. until the thickness of the stack reached approximately 2.5 mm. Excess of the liquid from the sides of the stack was removed by wiping. The sample consisted of a stack of ca 22 glass plates with the liquid between them, placed in a rectangular, sealed glass tube. The mean spacing between glass plates was estimated by weighing the introduced EAN, which yielded $d \sim 3.8$–$4.5$ μm [35]. A detailed description of the sample preparation and characterization has been reported in our previous paper [35]. To allow equilibration of ILs inside the samples, experiments were performed within a time from a week but not later than one and a half months after the sample preparation. The sample under study is anisotropic. We studied diffusion along glass plates and along the static magnetic field $\mathbf{B_0}$ of the NMR spectrometer when the sample was placed in a proper way in the probe. The sample was connected to the standard 5-mm NMR tube holder (spinner) without rotation of the spinner.

### 2.2. Pulsed-field gradient NMR diffusometry

NMR self-diffusion measurements were performed using a Bruker Ascend/Aeon WB 400 (Bruker BioSpin AG) NMR spectrometer with a resonance frequency of 400.27 MHz for $^1$H, 155.56 MHz for $^7$Li, and 40.56 MHz for $^{15}$N. Magnetic field strength was 9.4 T using a Diff50 Pulsed-Field-Gradient (PFG) probe. The diffusional decays (DDs) were recorded using the stimulated echo (StE) pulse trains. For single-component diffusion, the form of the DD can be described as [43,44]:

$$A(\tau, \tau_1, g, \delta) \propto \exp\left(-\frac{2\tau}{T_2} - \frac{\tau_1}{T_1}\right)\exp(-\gamma_2\delta_2 g_2 D t_d) \quad (1)$$

Here, $A$ is the integral intensity of the NMR signal, $\tau$ and $\tau_1$ are the time intervals in the pulse train; $\gamma$ is the gyromagnetic ratio for protons; $g$ and $\delta$ are the amplitude and the duration of the gradient pulse; $t_d = (\Delta - \delta/3)$ is the diffusion time; $\Delta = (\tau + \tau_1)$. $D$ is the diffusion coefficient. In the measurements, the duration of the 90° pulse was 7 μs, $\delta$ was in the range of $(0.5 \div 2)$ ms, $\tau$ was in the range of $(3 \div 5)$ ms, and $g$ was varied from 0.06 up to 29.73 T·m$^{-1}$. Diffusion time $t_d$ was varied from 4 to 500 ms. The recycle delay during accumulation of signal transients was 3.5 s. Data were processed using Bruker Topspin 3.5 software. Non-linear least squares regression was used to fit the experimental data with Eq. (1) to extract $D$ values.

### 2.3. Ionic conductivity

A Metrohm Autolab PGSTAT302N electrochemical workstation with an FRA32M module was used for ionic conductivity measurements using a Nova 2.02 software. The ionic conductivities were measured in the frequency range from 1 Hz to 1 MHz using 10 $mV_{rms}$ AC voltage amplitude. A two-electrode set-up was used with a 0.25 mm platinum wire as a working electrode and a 70 μL Pt cup as a sample container and as a counter electrode. Prior to each experiment, both the electrodes were polished with a Kemet diamond paste 0.25 μm. The cell constant was determined by using a 100 μS cm$^{-1}$ KCl standard solution from Metrohm (Kcell = 18.5396 cm$^{-1}$). The cell was thermally equilibrated for 10 min before each measurement.

## 3. Results and discussion

### 3.1. Bulk systems

$^1$H NMR spectra of EAN and $LiNO_3$ mixtures demonstrate three peaks corresponding to the protons of —$NH_3$, —$CH_2$— and —$CH_3$ chemical groups of the ethylammonium cation [26,35]. The addition of $LiNO_3$ to EAN results in shifting of the $^1$H resonance line corresponding to —$NH_3$ group to higher field and causes a slight broadening of lines corresponding to all other groups, Figs. S1, S2 in the Electronic Supporting Information, (ESI), which is in accordance with the previous observations [26]. This means that shielding of the protons in —$NH_3$ group at room temperature progressively increases with an increase in the fraction of the added salt. The line broadening corresponding to the —$NH_3$ protons is related with a decrease in the reorientational mobility of the cation. This can be related with an increase in the mean number of $NO_3^-$ anions near the —$NH_3$ group. This agrees with the disruption effect of inorganic cations offering on polar region of an IL, which leads to the formation of N-$H_N$...O hydrogen bonds between the cation and anion [26]. The monotonous change in the —$NH_3$ chemical shift reverses at concentrations of $LiNO_3$ between 10 and 15 wt%. A similar effect has been observed previously in the mixture of $[Pyr_{1201}][TFSI]$ with Li[TFSI] at low concentrations of the lithium salt [29]. This trend can be explained by a variation of the side groups coordinating to the $Li^+$ ion in different Li concentration regimes. The $^7$Li NMR spectrum presents a single resonance line corresponding to the $Li^+$ ion (Fig. S3).

#### 3.1.1. Diffusivity in bulk EAN/$LiNO_3$ mixtures

$^1$H and $^7$Li NMR diffusional decays are of single-component form (Eq.(1)). Diffusion coefficients of ethylammonium cation ($EA^+$) as well as $Li^+$ ion, calculated from slopes of the corresponding diffusion decays are comparable to each other and decrease proportionally with an increase in the concentration of the added salt (Fig. 1). A comparable diffusion of $EA^+$ and $Li^+$ was also observed in the previous study by Matveev *et al.* [26]. The phenomenon that diffusivity of $Li^+$ is comparable to that of organic cation is different from that observed in aprotic ILs with added lithium salts, where the diffusion coefficient of $Li^+$ was significantly lower than those of other organic and inorganic ions [45–49]. The effect of decreased diffusivity of $Li^+$ in the mixtures with aprotic and protic ILs was also demonstrated by simulations [50]. This is also quite unusual bearing in mind that $D$ of the nitrate anion in neat EAN is a factor of ~ 1.4 higher than that of $EA^+$ cation. We additionally measured diffusion of the $^{15}$N enriched nitrate anion in EAN/$LiNO_3$ mixture with 7.6 mol% of $LiNO_3$. $D$ of $EA^+$ cation was ~ $3.2{\cdot}10^{-11}$ m$^2$/s and $D$ of anion was ~ $5.0{\cdot}10^{-11}$ m$^2$/s. Therefore, the ratio of diffusivities of the nitrate anion to $EA^+$ cation was almost the same as in the neat EAN. It is known that the neat EAN exhibits an inherent

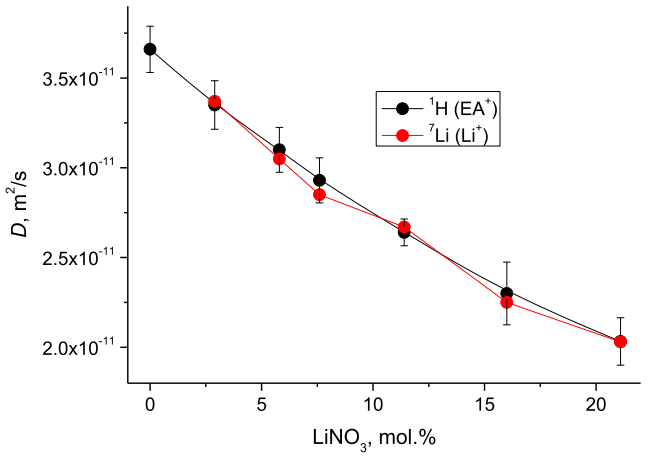


**Fig. 1.** Diffusion coefficients for $EA^+$ cation and $Li^+$ as a function of the $LiNO_3$ concentration at 298 K.

amphiphilic nanostructure in the liquid state, as it was suggested by small-angle neutron scattering and NMR diffusometry [20,35]. Molecular view of the dynamics in the system, which agrees with NMR diffusion data [35] is as follows. Several $EA^+$ cations are linked because of the hydrophobic interactions in an associate, which also contains anions electrostatically interacting with cations. The diffusion of cations is determined by the size of the associate. However, the anions are individually exchanging between associates during diffusion time of the NMR PFG experiment. Therefore, the measured diffusion coefficients of the anions are higher than the cations. From equality of the diffusion coefficients of $Li^+$ and $EA^+$, it is suggested that the added $Li^+$ ions are going in the existing associates and decrease their diffusivity by increasing either of the associate size or/and the lifetime of the cation in the associates.

The temperature dependences of the diffusion coefficients of $EA^+$ and $Li^+$ are shown in Arrhenius plots in Figs. 2 and 3, respectively. The dependences have a convex form that is typical for various ILs [45,51]. This was also observed previously for $EA^+$ [35,52]. Usually, such type of dependences can be described well by a Vogel-Fulcher-Tammann (VFT) equation in the form for diffusivity [45,51]:

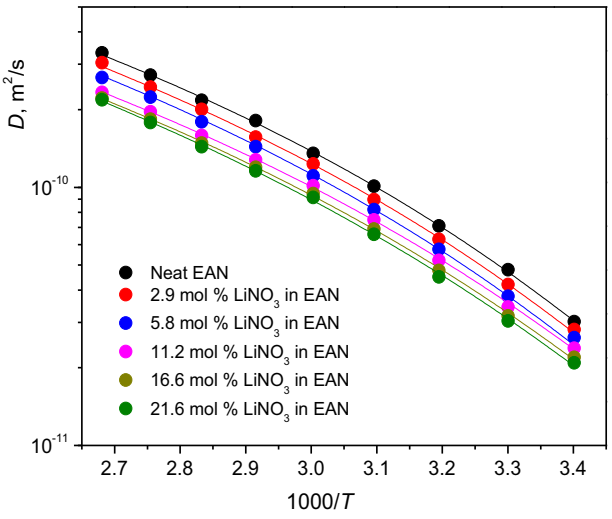


**Fig. 2.** Arrhenius plots of diffusivity of the $EA^+$ cation in EAN/$LiNO_3$ mixtures with different concentrations of $LiNO_3$ measured by $^1H$ NMR.

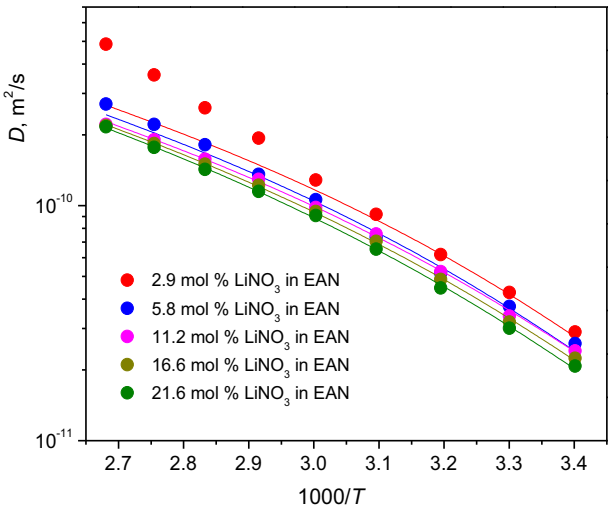


**Fig. 3.** Arrhenius plots of diffusivity of the $Li^+$ in EAN/$LiNO_3$ mixtures with different concentrations of $LiNO_3$ measured by $^7Li$ NMR.

$$D = D_0 \exp\left(\frac{-B}{(T - T_0)}\right) \quad (2)$$

where $D_0$, $T_0$, $B$ are adjustable parameters. $T_0$ is the dynamic (ideal) glass transition temperature, which is usually bellow the glass transition temperature determined by mechanical methods and depends on the applied frequency in the used technique, particularly NMR. Energy of activation for diffusion is related with $B$ as $E_D = B \cdot R$. We described dependences $D(T)$ for $EA^+$ and $Li^+$ in Figs. 2 and 3 by fitting Eq. (2) using appropriate fitting parameters $D_0$, $T_0$ and $B$. The best results of these fittings are shown by solid lines in the figures. As it is seen, VFT approach fits most of the dependences very well, except the diffusivities of $Li^+$ in the mixtures with lower $LiNO_3$ concentrations 2.9 and 5.8 mol%. For these concentrations, we used only low-temperature range of the temperature dependences for fitting due to several reasons, which will be explained later in the paper. The parameters of the fitting and calculated activation energies of diffusion are presented in Table 1.

As it is clear from Figs. 2 and 3, an increase in the $LiNO_3$ concentration leads to a decrease in the diffusion coefficients of $EA^+$ and $Li^+$ in the whole range of temperatures and not only at 298 K (Fig. 1). The dynamic glass transition temperature $T_0$ changes only slightly. The increase in $LiNO_3$ concentration leads to a monotonous increase in the activation energy for $EA^+$ diffusivity by a factor of 1.17 in comparison with the neat EAN. $E_D$ of $EA^+$ is slightly higher than that of the $Li^+$ at the same concentration of $LiNO_3$. This might be related with the free reorientation of the smaller $Li^+$ ion, because of the reorientation of molecules influencing mechanisms of their diffusivities.

It is important to mention that the properties of EAN/$LiNO_3$ mixtures at such low concentrations of $LiNO_3$ (less 6 mol%) are not investigated previously. For lower concentrations of $LiNO_3$ (2.9 and 5.8 mol%), the diffusion coefficients of $Li^+$ at higher part of temperature range of the study are different from $D$ of $EA^+$ and the corresponding temperature dependences deviate from the common trends as observed for $EA^+$ in neat EAN and mixtures with higher concentrations of the salt (Fig. 3). The added $Li^+$ ions built up in the existing associates formed by $EA^+$ cation at lower temperatures. Further, the addition of thermal energy with heating evidently allows $Li^+$ ions to separate from the associates and diffuse independently.

**Table 1**
VFT equation parameters and apparent activation energies of ion diffusivity for EAN/$LiNO_3$ mixtures with different concentrations of $LiNO_3$.

| $LiNO_3$, mol% | ion | $D_0 \times 10^{-9}$ $m^2/s$ | B,K | $T_0$, K | $E_D$, kJ/(mol) |
|---|---|---|---|---|---|
| 0 | $EA^+$ | 6.59 ± 0.03 | 538 ± 3.9 | 194 ± 4 | 4.47 ± 0.03 |
| 2.9 | $EA^+$ | 6.30 ± 0.04 | 555 ± 5.1 | 192 ± 4 | 4.61 ± 0.03 |
| | $Li^+$ | 5.00 ± 0.21 | 530 ± 28 | 192 ± 4 | 4.41 ± 0.23 |
| 5.8 | $EA^+$ | 6.20 ± 0.04 | 570 ± 4.9 | 191 ± 4 | 4.74 ± 0.04 |
| | $Li^+$ | 5.00 ± 0.11 | 550 ± 15 | 191 ± 4 | 4.57 ± 0.12 |
| 11.2 | $EA^+$ | 5.10 ± 0.03 | 570 ± 4.8 | 188 ± 4 | 4.74 ± 0.04 |
| | $Li^+$ | 4.70 ± 0.05 | 560 ± 7.1 | 188 ± 4 | 4.66 ± 0.06 |
| 16.6 | $EA^+$ | 5.35 ± 0.04 | 596 ± 5.2 | 186 ± 4 | 4.96 ± 0.03 |
| | $Li^+$ | 5.21 ± 0.04 | 591 ± 5.7 | 186 ± 4 | 4.91 ± 0.05 |
| 21.6 | $EA^+$ | 5.98 ± 0.05 | 631 ± 6.4 | 183 ± 4 | 5.25 ± 0.05 |
| | $Li^+$ | 5.93 ± 0.04 | 631 ± 6.4 | 183 ± 4 | 5.25 ± 0.05 |

### 3.1.2. Ionic conductivity of EAN/$LiNO_3$ mixtures

Generally, the addition of lithium salt leads to a monotonous decrease in ionic conductivity and ion diffusivity of the electrolytes due to the stronger Coulomb interactions. On the contrary, we observed two different types of temperature dependences depending on the concentration of the Li-salt in the EAN. (a) The mixtures with lower concentration of $LiNO_3$ (up to ~ 6 mol%) showed unusual behaviour and (b) the neat EAN as well as the mixtures with concentrations of the $LiNO_3$ higher than 6 mol% The representative Arrhenius plots of the experimental values of ionic conductivities for the mixtures with lower (type a) and higher (type b) concentrations of $LiNO_3$ are shown by symbols in Figs. 4 and 5, respectively. The temperature dependences for the mixtures with higher concentrations of $LiNO_3$ shows a typical convex form (Fig. 5), similar to the previously obtained ionic conductivity data for aprotic ILs [45–49,51] and neat EAN [35,52]. The ionic conductivity values obtained during heating and cooling cycles of these systems are perfectly matching and overlapping.

The Vogel-Fulcher-Tammann (VFT) equation is used typically for the convex form of ionic conductivity in Arrhenius coordinates:

$$\sigma = \sigma_0 \exp\left(\frac{-B}{(T - T_0)}\right) \quad (3)$$

where $\sigma_0$, $B$, and $T_0$ are the fitting parameters: pre-exponential factor, a factor related to the activation energy and the ideal glass transition temperature, respectively. The activation energy for ionic conductivity is related with $B$ as $E_\sigma = B{\cdot}R$. The temperature dependence of ionic conductivity for the neat EAN and the EAN/$LiNO_3$ mixtures with higher concentrations of $LiNO_3$ are fitted well to the VFT model over the whole studied temperature range (Fig. 5, lines). The VFT parameters for the ionic conductivity are summarized in Table 2. As it is seen, the addition of $LiNO_3$ slightly influences the $T_0$, while $E_\sigma$ increases by a factor ~ 1.1. the pre-exponential factor $\sigma_0$ increases with the addition of $LiNO_3$ (due to an increase in the charge carriers) that should increase ionic conductivity. However, the addition of $LiNO_3$ lead to a decrease in the ionic conductivity; evidently, this process is controlled by an increase in the energy barrier ($E_\sigma$). An increase in $E_\sigma$ as well as $E_D$ was observed in most of studied IL with the addition of inorganic salts that is conditioned by alteration of the inter-ion interactions.

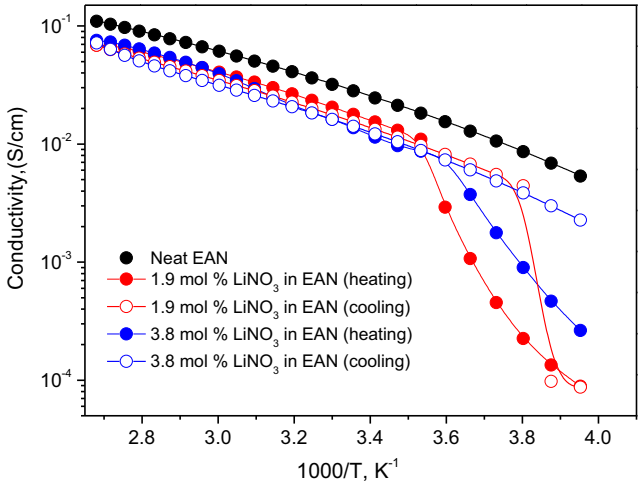


**Fig. 4.** Arrhenius plots of ionic conductivities of the neat EAN and the EAN/$LiNO_3$ mixtures with different $LiNO_3$ concentrations (symbols and connecting lines).

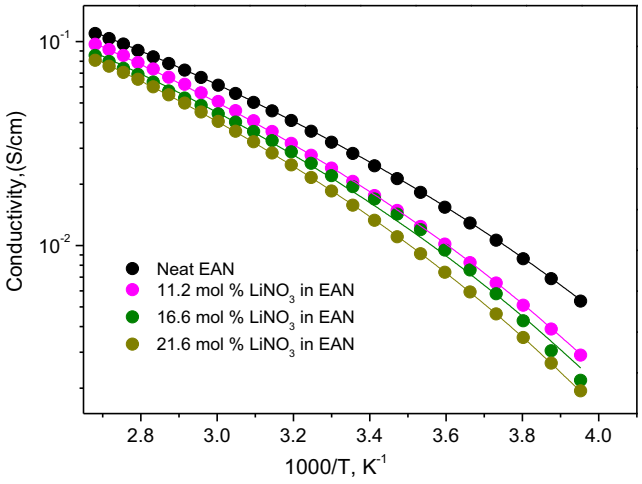


**Fig. 5.** Arrhenius plot of ionic conductivity for the neat EAN and the EAN/$LiNO_3$ mixtures with different concentrations of $LiNO_3$ (symbols), and their best fittings using VFT equation (lines).

The dependence of ionic conductivity on the molecular (ionic) mobility of ions in a system has a complex mechanism. Therefore, it is not surprising that the parameters obtained from the temperature dependences of $\sigma(T)$ and $D(T)$ are different. The range of $T_0$ for ionic conductivity is lower by ~ 50 K. The ion diffusivity is measured in equilibrium conditions while ionic conductivity measurements are performed under the application of an external electrical potential and frequency. This might decrease the energy barrier as compared with the case of an equilibrium condition.

In case of the mixtures with lower concentrations of $LiNO_3$, the ionic conductivity data during the heating and cooling cycles do not coincide demonstrating a type of hysteresis (Fig. 4). During the heating process, the ionic conductivity at lower temperatures is ~ 2 decimal order lower than for the neat EAN. An increase in the temperature leads to an abrupt recovery of the ionic conductivity values to the "normal" form. The temperature of the transition shifts to lower temperatures as the concentration of the $LiNO_3$ increases. Generally, a decrease in ionic conductivity can be condi-

**Table 2**
VFT equation parameters and energies of activation for the ionic conductivity data for the neat EAN and the EAN/$LiNO_3$ mixtures with higher concentrations of the $LiNO_3$ salt.

| $LiNO_3$, mol% | $\sigma_0$ S/cm | $B$, K | $T_0$, K | $E_\sigma$, kJ/(mol) |
|---|---|---|---|---|
| 0 | 2.001 ± 0.003 | 680 ± 0.51 | 138 ± 5 | 5.65 ± 0.004 |
| 11.2 | 2.378 ± 0.007 | 725 ± 1.2 | 145 ± 5 | 5.99 ± 0.01 |
| 16.6 | 2.136 ± 0.048 | 720 ± 7.5 | 146 ± 5 | 5.99 ± 0.06 |
| 21.6 | 2.272 ± 0.005 | 750 ± 0.88 | 147 ± 5 | 6.24 ± 0.007 |

tioned by a decrease in the number of charged particles (ions) or a decrease in their mobility. A decrease in mobility of ions at lower temperatures can be related with the sample solidification (vitrification or crystallization). This is not the case of EAN/$LiNO_3$ mixtures, which remains in liquid state in the whole range of $LiNO_3$ concentrations and the studied temperatures, as it evident from the diffusivity data (Figs. 1–3). On the other hand, a decrease in the amount of charged particles can be conditioned by a decrease in the degree of dissociation of EAN in the presence of $LiNO_3$. Further an increase in temperature to the higher-temperature range leads to a partial "liberation" of the $Li^+$ ions that recovers dissociation of EAN and the "normal" form of the temperature dependence of $\sigma(T)$, as shown in Fig. 3. Keeping this suggestion in mind, stoichiometry of the low-dissociating complex is nearly $(EA^+):(Li^+):(NO_3^-) \sim 0.485:0.015:0.5$. Therefore, the formation of complexes (associates) in the EAN/$LiNO_3$ mixture is in accordance with the previous studies [15,26,29]. A change in the dynamics and the associated structure of EAN induced by $Li^+$ ions is previously observed by electrophoretic NMR [29], where the $Li^+$ remained in a negatively charged complexes.

Therefore, the increase in the concentration of $LiNO_3$ in EAN effects the ion diffusivity and the ionic conductivity differently and depends on the Li-salt concentration and the temperature range. An increase in the Li-salt concentration leads to a decrease in the diffusivity and ionic conductivity of $EA^+$ and $Li^+$. In the case of the neat EAN and the mixtures with Li-salt concentrations higher than 6 mol %, there is a common form of temperature dependences. As expected, an increase in the Li-salt concentration leads to an increase in the activation energies for diffusion and ionic conductivity. For the salt concentrations lower than 6 mol %, there are anomalies in ion diffusivity of $Li^+$ in the high-temperature range and for ionic conductivity in the low-temperature range. These anomalies can be explained by the formation of low-dissociating complexes at lower temperatures and liberation of $Li^+$ leading to recovery of the charge at higher temperatures.

### 3.2. EAN/$LiNO_3$ mixture enclosed between glass plates

Fig. 6 shows the diffusion coefficients of $EA^+$ cation and $Li^+$ ion in the EAN/$LiNO_3$ mixture enclosed between glass plates as a function of time exposed to a magnetic field of the NMR spectrometer. The diffusion coefficient of $EA^+$ just after placement of the sample in the magnetic field (solid circles) is higher by a factor of ~ 2.5 as compared with the bulk diffusion coefficient (dotted line). A similar trend is previously observed for neat EAN enclosed between glass plates [35]. The diffusivity of $Li^+$ (open circles) follows the same trend as the $EA^+$ cation and demonstrating higher diffusivity than in the bulk. This was recently explained by weakening of the hydrogen bonding network in the neat EAN, as evident by an upfield shift of the chemical shifts of $-NH_3$ protons [52].

A long time exposure of the sample to magnetic field leads to a gradual decrease in the diffusivities of both $EA^+$ and $Li^+$ until they reach equilibrium values, which are comparable to the bulk diffusivities. A similar process was observed earlier for enclosed neat EAN [38], propylammonium [41] and 1-ethyl-3-methyl imidazolium [40] having nitrate as an anion. This process is reversible

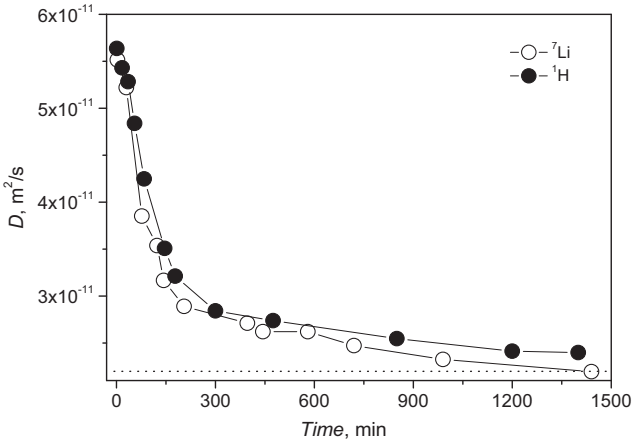


**Fig. 6.** Evolution of diffusion coefficients of ethylammonium cation (solid circles) and $Li^+$ (open circles) in the mixture of EAN and $LiNO_3$ containing 15 mol% of $LiNO_3$ enclosed between glass plates in a magnetic field of 9.4 T/m. The time scale started at the time moment of placing of the sample in the magnetic field. The temperature of this experiment is constant at T = 295 K. Dashed line corresponds to the diffusion of ions in the bulk mixture at the same conditions of measurements.

and follows the equation of Avramís kinetics [41]; the fact which was used to propose a phase transformation occurring in the enclosed nitrate-based ILs under the influence of magnetic field [41].

This observation shows that the dynamics of $Li^+$ ion and transformation occurring in the enclosed EAN/$LiNO_3$ system is similar to those of enclosed neat EAN and other nitrate-based ILs with different organic cations. Therefore, such peculiarities of this and other similar ILs are conditioned mainly by the presence of the nitrate anion.

## 4. Conclusions

The diffusivity of ions and ionic conductivity in EAN/$LiNO_3$ mixtures as a function of concentration of lithium salt and temperature are measured. The diffusion decays obtained for $EA^+$ cation and $Li^+$ ion are single-component in form. It is revealed that there are two ranges of concentrations and temperatures where the diffusivity of ions and the ionic conductivities behave in an unusual manner. In the low-temperature range, the diffusivities of $EA^+$ and $Li^+$ coincide, and demonstrate a gradual decrease in ion diffusivity as the concentration of $LiNO_3$ increases. This is very different from most of the studied protic and aprotic ILs, where diffusivity of $Li^+$ is much lower than the organic ions. An analysis of the NMR spectra showed that the mean number of anions near the amino group of the cation increases, and ions of lithium build up in the structure of the associates formed by hydrophobic chains of the $EA^+$ cations. At lower concentration of the $LiNO_3$ salt (less than 6 mol. %), the ionic conductivity of the system is significantly lower than the expected values, due to the lower degree of dissociation of the associates formed by ions. Hysteresis for the ionic conductivity in the heating–cooling cycles is observed in this concentration range. For the system with the lithium salt concentration higher than

6 mol % no such anomalies are observed, and an expected trend is observed with increasing Li-salt concentration.

In the higher temperature range, the ionic conductivities and diffusion of $EA^+$ over the whole concentrations range, and the diffusion of $Li^+$ at the higher concentrations range demonstrate a monotonous decrease with an increase in the concentration of $Li^+$. However, for the lower concentration range, the diffusivity $Li^+$ exceeded the diffusivity of the $EA^+$ cation that demonstrates the release of $Li^+$ from the associates. The diffusivities of $EA^+$ and $Li^+$ for the system enclosed between glass plates showed peculiarities similar to the earlier observed in other neat nitrate-based ILs: accelerated diffusivity of cations and reversible alteration of the diffusivities under the influence of strong static magnetic field. Keeping in mind the potential applications of ILs including EAN in electrochemical devices, this study can find interest among researchers working in this field.

## CRediT authorship contribution statement

**Andrei Filippov:** Conceptualization, Methodology, Investigation, Writing - original draft. **Artem S. Alexandrov:** Investigation, Software. **Rustam Gimatdinov:** Software, Data curation. **Faiz Ullah Shah:** Investigation, Validation, Writing - review & editing.

## Declaration of Competing Interest

The authors declare that they have no known competing financial interests or personal relationships that could have appeared to influence the work reported in this paper.

## Acknowledgements

The financial support from the Swedish Research Council (project number: 2018-04133) is gratefully acknowledged for supporting this work. A.S.A. acknowledges the subsidy allocated to the Kazan Federal University for the state assignment in the sphere of scientific activities (project number: 0671-2020-0051).

## Appendix A. Supplementary material

Supporting information is available having $^1H$ solution NMR spectra of EAN/$LiNO_3$ spectra for the system with varied concentration of $LiNO_3$, alteration of chemical shift in the system and $^7Li$ NMR spectrum of the mixture. Supplementary data to this article can be found online at https://doi.org/10.1016/j.molliq.2021.116841.

## References

[1] R.D. Rogers, K.R. Seddon, Ionic liquids-solvents of the future?, Science 302 (2003) 792–793.
[2] T.L. Greaves, C.J. Drummond, Protic ionic liquids: properties and applications, Chem. Rev. 108 (2008) 206–237.
[3] N.V. Plechkova, K.R. Seddon, Applications of ionic liquids in the chemical industry, Chem. Soc. Rev. 37 (2008) 123–150.
[4] M. Smiglak, J.M. Pringle, X. Lu, L. Han, S. Zhang, H. Gao, D.R. MacFarlane, R.D. Rogers, Ionic liquids for energy, materials, and medicine, Chem. Commun. 50 (2014) 9228–9250.
[5] M. Armand, F. Endres, D.R. MacFarlane, H. Ohno, B. Scrosati, Ionic-liquid materials for the electrochemical challenges of the future, Nat. Mater. 8 (2009) 621–629.
[6] R. Zarrougui, M. Dhahbi, D. Lemordant, Transport and thermodynamic properties of ethylammonium nitrate–water binary mixtures: effect of temperature and composition, J. Solution Chem. 44 (2015) 686–702.
[7] P. Walden, Über die Moleculargröße und Elektrische Leitfähigkeit Einiger Geschmolzener Salze, Bull. Acad. Imp. Sci. St Petersburg 8 (1914) 405–422.
[8] J.A. Garlitz, C.A. Summers, R.A. Flowers, G.E. Borgstahl, Ethylammonium nitrate: a protein crystallization reagent, Acta Crystallogr. D: Biol. Crystallogr. 55 (1999) 2037–2038.
[9] C.A. Summers, R.A. Flowers, Protein renaturation by the liquid organic salt ethylammonium nitrate, Protein Sci. 9 (2000) 2001–2008.
[10] D.F. Evans, A. Yamauchi, R. Roman, E.Z. Casassa, Micelle formation in ethylammonium nitrate, a low-melting fused salt, J. Colloid Interface Sci. 88 (1982) 89–96.
[11] Y. Huang, G. Zhou, Y. Li, Z. Yang, M. Shi, X. Wang, X. Chen, F. Zhang, W. Li, Molecular dynamics simulations of temperature-dependent structures and dynamics of ethylammonium nitrate protic ionic liquid: The role of hydrogen bond, Chem. Phys. 472 (2016) 105–111.
[12] R. Hayes, G. Warr, R. Atkin, Structure and nanostructure in ionic liquids, Chem. Rev. 115 (2015) 6357–6426.
[13] A. Kachmar, M. Carignano, T. Laino, M. Iannuzzi, J. Hutter, Mapping the free energy of lithium solvation in the protic ionic liquid ethylammonuim nitrate: A metadynamics study, ChemSusChem 10 (2017) 3083–3090.
[14] C.A. Gunawan, B.H.R. Suryanto, C. Zhao, Electrochemical Study of Copper in Room Temperature Protic Ionic Liquids Ethylammonium Nitrate and Triethylammonium Methylsulfonate, J. Electrochem. Soc. 159 (10) (2012) D611–D615.
[15] O. Russina, R. Caminita, T. Mendez-Morales, J. Carrete, O. Cabeza, L.J. Gallego, L. M. Varela, A. Triolo, How does lithium nitrate dissolve in a protic ionic liquid?, J. Molec. Liq. 205 (2015) 16–21.
[16] K. Fumino, S. Reimann, R. Ludwig, Probing molecular interaction in ionic liquids by low frequency spectroscopy: Coulomb energy, hydrogen bonding and dispersion forces, Phys. Chem. Chem. Phys. 16 (2014) 21903–21929.
[17] R. Hayes, S. Imberti, G.G. Warr, R. Atkin, Amphiphilicity determines nanostructure in protic ionic liquids, Phys. Chem. Chem. Phys. 13 (2011) 3237–3247.
[18] Y. Umebayashi, W.-L. Chung, T. Mitsugi, S.h. Fukuda, M. Takeuchi, K. Fujii, T. Takamuku, R. Kanazaki, S.-I. Ishiguro, Liquid structure and the ion-ion interactions of ethylammonium nitrate ionic liquid studied by large angle X-ray scattering and molecular dynamics simulations, J. Comp. Chem. Japan 7 (2008) 125–134.
[19] T. Zentel, V. Overbeck, D. Michalik, O. Kühn, R. Ludwig, Hydrogen bonding in protic ionic liquids: structural correlations, vibrational spectroscopy, and rotational dynamics of liquid ethylammonium nitrate, J. Phys. B: Atomic, Mol. Optic. Phys. 51 (2018) 151–168.
[20] R. Atkin, G.G. Warr, The smallest amphiphiles: nanostructure in protic room-temperature ionic liquids with short alkyl groups, J. Phys. Chem. B 112 (2008) 4164–4166.
[21] Y. Litaeim, M. Dhahbi, Measurements and correlation of viscosity and conductivity for the mixtures of ethylammonium nitrate with organic solvents, J. Molec. Liq. 155 (2010) 42–50.
[22] A.B. Pereiro, J.M.M. Araújo, F.S. Oliveira, C.E.S. Bernardes, J.M.S.S. Esperança, J. N. Canongia Lopes, I.M. Marrucho, L.P.N. Rebelo, Inorganic salts in purely ionic liquid media: the development of high ionicity ionic liquids (HIILs), Chem. Commun. 48 (2012) 3656–3658.
[23] B. Garcia, S. Lavallée, G. Perron, C. Michot, M. Armand, Room temperature molten salts as lithium battery electrolyte, Electrochim. Acta 49 (2004) 4583–4588.
[24] M.Y. Lui, L. Crowhurst, J.P. Hallett, P.A. Hunt, H. Niedermeyer, T. Welton, Salts dissolved in salts: ionic liquid mixtures, Chem. Sci. 2 (2011) 1491–1496.
[25] N. Hjalmarsson, R. Atkin, M.W. Rutland, Effect of lithium ions on rheology and interfacial forces in ethylammonium nitrate and ethanolammonium nitrate, J. Phys. Chem. C 120 (2016) 26960–26967.
[26] V.V. Matveev, A.V. Ievlev, M.A. Vovk, O. Cabeza, J. Salgado-Carballo, J.J. Parajó, J. R. Rodríguez, R. de la Fuente, E. Lähderanta, L.M. Varela, NMR investigation of the structure and single-particle dynamics of inorganic salt solutions in a protic ionic liquid, J. Molec. Liq. 278 (2019) 239–246.
[27] J.S. Lee, J.Y. Bae, H. Lee, N.D. Quan, H.S. Kim, H. Kim, Ionic liquids as electrolytes for Li ion batteries, J. Ind. Eng. Chem. 10 (2004) 1086–1089.
[28] T. Mendez-Morales, J. Carrete, J.R. Rodriguez, O. Cabeza, L.J. Gallego, O. Russina, L.M. Varela, Nanostructure of mixtures of protic ionic liquids and lithium salts: effect of alkyl chain length, Phys. Chem. Chem. Phys. 17 (2015) 5298–5307.
[29] M. Brinkkötter, A. Mariani, S. Jeong, S. Passerini, M. Schönhoff, Ionic liquids in Li salt electrolyte: Modifying the $Li^+$ transport mechanism by coordination to an asymmetric anion, Adv. Energy Sustainability Res. 2 (2020) 2000078.
[30] N. Molinari, J.P. Mailoa, B. Kozinsky, General Trend of a Negative Li Effective Charge in Ionic Liquid Electrolytes, J. Phys. Chem. Lett. 10 (2019) 2313–2319.
[31] S.h. Zhang, J. Zhang, Y. Zhang, Y. Deng, Nanoconfined ionic liquids, Chem. Rev. 117 (2017) 6755–6833.
[32] M.A. Gebbie, A.M. Smith, H.A. Dobbs, A.A. Lee, G.G. Warr, X. Banquy, M. Valtiner, M.W. Rutland, J.N. Israelachvili, S. Perkin, R. Atkin, Chem. Commun. 53 (2017) 1214–1224.
[33] C. Iacob, J.R. Sangoro, W.K. Kipnusu, R. Valiullin, J. Kärger, F. Kremer, Enhanced charge transport in nano-confined ionic liquids, Soft Matter 8 (2012) 289–293.
[34] S.M. Chathoth, E. Mamontov, P.F. Fulvio, X. Wang, G.A. Baker, S. Dai, D.J. Wesolowski, An unusual slowdown of fast diffusion in a room temperature ionic liquid confined in mesoporous carbon, Europhys. Lett. 102 (2013) 16004.
[35] A. Filippov, O.I. Gnezdilov, N. Hjalmarsson, O.N. Antzutkin, S. Glavatskih, I. Furó, M.W. Rutland, Acceleration of diffusion in ethylammonium nitrate ionic liquid confined between parallel glass plates, Phys. Chem. Chem. Phys. 19 (2017) 25853–25858.
[36] A. Filippov, N. Azancheev, F.U. Shah, S. Glavatskih, O.N. Antzutkin, Self-diffusion of phosphonium bis(salicylato)borate ionic liquid in pores of Vycor porous glass, Micropor. Mesopor. Mater. 230 (2016) 128–134.

[37] A. Filippov, O.N. Antzutkin, F.U. Shah, Rapid carbene formation increasing ion diffusivity in an imidazolium acetate ionic liquid confined between polar glass plates, Phys. Chem. Chem. Phys. 21 (2019) 22531–22538.
[38] A. Filippov, O.N. Antzutkin, Magnetic field effects dynamics of ethylammonium nitrate ionic liquid confined between glass plates, Phys. Chem. Chem. Phys. 20 (2018) 6316–6320.
[39] A. Filippov, S. Kurakin, O.I. Gnezdilov, O.N. Antzutkin, Effect of magnetic field on diffusion of ethylammonium nitrate – water mixtures confined between polar glass plates, J. Mol. Liq. 274 (2019) 45–51.
[40] A. Filippov, O.N. Antzutkin, R. Gimatdinov, O.I. Gnezdilov, Self-diffusion in ionic liquids with nitrate anion: effects of confinement between glass plates and static magnetic field, J. Mol. Liq. 312 (2020) 113404.
[41] A. Filippov, O.I. Gnezdilov, O.N. Antzutkin, Static magnetic field alters properties of confined alkyammonium nitrate ionic liquids, J. Mol. Liq. 268 (2018) 49–54.
[42] A. Filippov, O.I. Gnezdilov, A.G. Luchkin, O.N. Antzutkin, Self-diffusion of ethylammonium nitrate ionic liquid confined between modified polar glasses, J. Mol. Liq. 284 (2019) 366–371.
[43] P.T. Callaghan, Principles of Nuclear Magnetic Resonance Microscopy, Clarendon, Oxford, 1991.
[44] E.O. Stejskal, J.E. Tanner, Spin diffusion measurements: Spin echoes in the presence of a time-dependent field gradient, J. Chem. Phys. 42 (1965) 288–292.
[45] I.A. Khan, O.I. Gnezdilov, A. Filippov, F.U. Shah, Ion transport and electrochemical properties of flourine-free lithium-ion battery electrolytes derived from biomass, ACS Sustainable Chem. Eng. (2021), https://doi.org/10.1021/acssuschemeng.1c00939.
[46] F.U. Shah, O.I. Gnezdilov, A. Filippov Ion dynamics in halogen-free phosphonium bis(salicylato)borate ionic liquid electrolytes for lithium-ion batteries, Phys. Chem. Chem. Phys. 19 (2017) 16721–16730.
[47] F.U. Shah, O.I. Gnezdilov, R. Gusain, A. Filippov, Transport and association of ions in lithium battery electrolytes based on glycol ether mixed with halogen-free orthoborate ionic liquid, Sci. Rep. 7 (2017) 16340.
[48] F.U. Shah, O.I. Gnezdilov, I.A. Khan, A. Filippov, N.A. Slad, P. Johansson, Oligoether carboxylate ionic liquid based fluorine-free electrolytes, J. Phys. Chem. B 124 (2020) 9690–9700.
[49] K. Hayamizu, S. Tsuzuki, S. Seki, Transport and Electrochemical Properties of Three Quaternary Ammonium Ionic Liquids and Lithium Salt Doping Effects Studied by NMR Spectroscopy, Chem. Eng. Data 59 (2014) 1944–1954.
[50] A.T. Nasrabadi, V. Ganesan, Structure and Transport Properties of Lithium-Doped Aprotic and Protic Ionic Liquid Electrolytes: Insights from Molecular Dynamics Simulations, J. Phys. Chem. B 123 (2019) 5588–5600.
[51] H. Tokuda, K. Hayamizu, K. Ishii, M.A.B.H. Susan, M. Watanabe, Physicochemical properties and structures of room temperature ionic liquids. 2. Variation of alkyl chain length in imidazolium cation, J. Phys. Chem. B 109 (2005) 6103–6110.
[52] O.I. Gnezdilov, A. Filippov, O.N. Antzutkin, R. Gimatdinov, Temperature dependence of $^{1}$H NMR chemical shifts and diffusivity of ethylammonium nitrate ionic liquid confined between glass plates, Magn. Reson. Imag. 74 (2021) 84–89.